Synthetic Metals 301 (2024) 117492

Contents lists available at ScienceDirect

Synthetic Metals

journal homepage: www.elsevier.com/locate/synmet

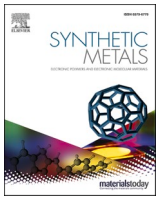

Electrochemical and radical properties of core-shell structure PDA@SiO_2

Krzysztof Tadyszak [*,1], Elena Tomšík [2], Zulfiya Černochová [3]

Institute of Macromolecular Chemistry, Czech Academy of Sciences, Prague, Czech Republic

ARTICLE INFO

Keywords:
Polydopamine
Silicon dioxide
Core-shell structure
Radical scavenging
EPR
Cyclic voltammetry

ABSTRACT

Radical and electrochemical properties of core-shell polydopamine structures (PDA@SiO_2) were studied. We have successfully covered large silica nanoparticles (ca. 960 nm) with a thin layer of polydopamine. The radical's concentration present in PDA is $1.32 \times 10^{15} spin/mg$ and after synthesis in PDA@SiO_2 system it is $8.4 \times 10^{13} spin/mg$. The core-shell structure maintained its radical scavenging properties due to a thin layer of PDA covering silica. Cyclic voltammetry (CV) shows a reduction of peak-to-peak potential separation and an increase of anodic and cathodic current with an increase in the scan rate. Electrochemical impedance spectroscopy shows the electrical connection between PDA and SiO_2. PDA@SiO_2 core-shell system is electrochemically non-degradable showing a quasi-reversible electrochemical response, which makes it a promising candidate for sensor applications.

1. Introduction

Core-shell structures have found applications in biology and chemistry due to their unique advantage of connecting best features of selected materials. These structures take advantage of combining metals, ceramics, or polymers in a single nanoplatform, to address problems of modern science and engineering. In this article, we have created SiO_2 particles covered by thin layer of PDA (PDA@SiO_2) as a nanostructure that can be used for further functionalization for applications in various fields. Unique properties of PDA allow to use it in tissue engineering [1], photocatalysis [2], drug delivery [3], immobilization of enzymes [4,5], hydrogel grafts [6], chemo- and photothermal therapy [7,8] due to its broad absorption band 200–700 nm [9], for H_2O_2 generation under 808 nm irradiation (pro-oxidant, radical-scavenging, antimicrobial activity) [10] EPR imaging [11], radical scavenging properties [10,12,13], it shows adhesive properties [14] towards noble metals, iron oxide [15] e.g. PDA was used as bonding agent for Au nanoparticles a sensor of dopamine, ascorbic acid, uric acid [16], and for energy storage [17], for improvements of cyclic stability using PDA@SiO_2 coating at $LiCoO_2$ cathode [6].

The unique feature of PDA is the presence of permanent quinone/semiquinone-like radicals [18] which appear during polymerization. At least two types of radicals were observed [19,20] having strongly overlapping EPR signals (similar g-factors ~2.003–2.004 [18,21]). The EPR line at X-band is slightly asymmetrical with the linewidth in the range 4–8 G [21,22] exhibiting spin concentration of 10^{16} - 10^{18} spin/g [23,24]. One of very interesting properties applicable in biology/medicine is a very potent radical scavenging feature. It is anticipated that ultra-small sized PDA particles will be superior in radical scavenging [13]. The EC_{50} value is ca. 27 μg of PDA NP's suspended in 1 ml of 100 μM DPPH EtOH (95 %) solution) [10]. Other authors mention this value as equal to ca. 17.5 μg/ml [25], 14 μg/ml [26].

In this article, we present core-shell nanoparticle structure PDA@SiO_2 where the core is a SiO_2 nanoparticle of the diameter of around ca. 960 nm and the shell consists of the polydopamine coating of ca. on average ~29 nm (measured by SEM), ~28 nm (TEM), ~50–80 nm (DLS). The electrochemical properties depend on the thickness of the PDA layer which is why we obtained a robust, stable core-shell structure model as a platform for ongoing studies.

2. Experimental

2.1. Core formation

Silicon oxide (SiO_2) nanoparticles were obtained by mixing 200 ml of EtOH with 25 ml of Milli-Q water and 64 ml of ammonium hydroxide

* Corresponding author.
E-mail address: tadyszak@imc.cas.cz (K. Tadyszak).
[1] 0000-0002-0370-9766.
[2] 0000-0002-1749-1091.
[3] 0000-0002-7119-7205.

https://doi.org/10.1016/j.synthmet.2023.117492
Received 9 August 2023; Received in revised form 6 October 2023; Accepted 24 October 2023
Available online 25 October 2023

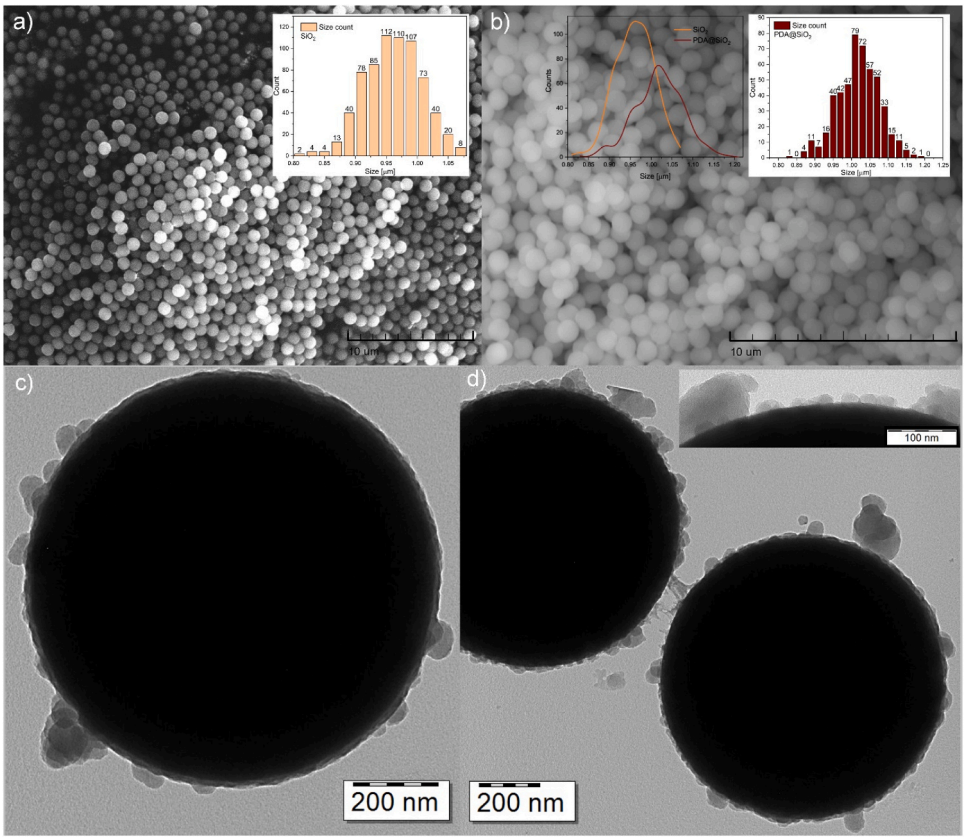

Fig. 1. a) SEM image of SiO_2 NPs – core; inset shows the size distribution; b) SEM image PDA@SiO_2 NPs; insets show the size distribution and transparent plot is the comparison of distributions SiO_2 – core and PDA@SiO_2 NPs. SEM scales 10 μm in both cases; c) and d) TEM image of single SiO_2 particles covered with PDA, inset shows a magnification of particle surface; TEM scales 200 nm, TEM inset 100 nm.

(NH_4OH, CAS No.: 1336–21–6, Merck). After 1 h of stirring 50 ml of tetraethyl orthosilicate (TEOS, CAS No.: 78–10–4, Merck) was added stepwise (few minutes). After 24 h of synthesis while stirring 250 rpm at 21 °C suspension was centrifugated at 9000 rpm. The resulting SiO_2 nanoparticles were precipitated and dried at 60 °C overnight.

2.2. Shell formation

25 mg of SiO_2 nanoparticles powder was grained in a mortar to a fine powder and further added to 5 ml of TRIS buffer of pH = 8.4 (100 mM, previously calibrated with formic acid, tris(hydroxymethyl)aminomethane, CAS No.: 17–1321–01, Merck). After 15 min ultrasonication 25 mg of dopamine hydrochloride was admixed (CAS No. 62–31–7 (Merck)). The concentration of dopamine was 5 mg/ml during the experiment. The polymerization reaction was taking place at 21 °C under vigorous stirring which took 48 h. After which nanoparticles suspension was centrifugated and the supernatant replaced with Milli-Q water for further dynamic light scattering - DLS, electron paramagnetic resonance spectroscopy - EPR, and electrochemical characterization by cyclic voltammetry (CV) and electrochemical impedance spectroscopy (EIS). Before measurement particles were dried at 60 °C overnight.

2.3. Electron paramagnetic resonance

The EPR measurements were conducted with Bruker ELEXSYS 540 X band spectrometer equipped with 049X microwave bridge (Super X), Bruker ER4108 TMHS slim design resonator. The following EPR spectrometer settings were applied for the experiments: microwave power: 6.45 mW (15 dB); modulation amplitude: 0.5 G; frequency modulation: 100 kHz; the time constant: 5.12 ms; conversion time: 20.48 ms; gain: 60 dB; resolution: 2048 points, temperature 294 K, usually 5 accumulations per spectrum, for SiO_2 radicals 50 accumulations were used. G-factors were estimated by comparison with DPPH free-radical standard assuming its g-factor equal to 2.0036. Spin concentration of the standard Al_2O_3:Cr^{3+} monocrystal which was placed on the side-wall of the resonator was estimated previous to the main experiment by calibration of with commercially available alanine spin concentration standard from Bruker (ER 213 ASC Alanine Spin Concentration Sample E3005324 – Ser. No. 201812-10; spin concentration 1.7×10^{17} spins).

Radical scavenging experiments were performed 1 h after mixing 100 μl DPPH (free radical - 2,2-diphenyl-1-picrylhydrazyl, CAS No.: 1898–66–4, Merck) solution (80/20 ethanol/TRIS pH = 8.4) with selected volumes of PDA (0.51 mg/ml) and PDA@SiO_2 (0.63 mg/ml) suspensions in the same liquid. Nanoparticle suspensions were 45 min ultrasonicated (low power) solely for homogenization before pipetting for main experiment. Ascorbic acid (CAS No. 50–81–7, Merck) was used as a standard sample (0.196 mg/ml in pure TRIS buffer pH = 8.4). After 1 h curation time, while vigorously stirring 20 μl of suspension was taken for EPR study.

2.4. Electrochemistry

Carbon rods Koh-i-noor 2 mm HB (CR) were from Neilsen s.r.o. Czech Republic and was cleaned with ethanol and distilled water before depositing PDA films.

Electrochemical characterization of electrodes (PDA deposited at carbon rods) was carried out by cyclic voltammetry (CV) in 0.3 M aq. NaCl electrolyte. The CV was performed at 25 °C in three electrodes cell configuration using an AUTOLAB PGSTAT302N potentiostat (Metrohm Inula GmbH, Prague, Czech Republic) with a FRA32M Module and Nova 2.1 software. A Pt sheet (1.2 cm^2) was used as the counter electrode, and the Ag/AgCl (3 M KCl) was applied as the reference electrode. The

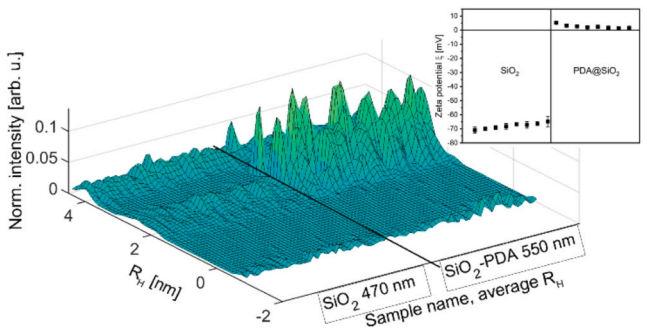

Fig. 2. The 3D scheme of DLS measurements of silica and PDA-covered silica particles at room temperature. The sample concertation was 0.1 mg/ml; inset zeta potential measurements at the same conditions.

potential sweeps were carried out between − 0.2 and 0.8 V vs. Ag/AgCl at variable scan rates.

The electrochemical impedance spectroscopy was measured at open circuit potential in three electrodes cell configuration using an AUTOLAB PGSTAT302N potentiostat (Metrohm Inula GmbH, Prague, Czech Republic) with a FRA32M Module and Nova 2.1 software, applying the frequency range from 10^{-1} to 10^{6} Hz with 5 mV perturbation.

2.5. Dynamic light scattering and zeta potential

Dynamic Light Scattering (DLS) and zeta potential measurements (ξ). We measured the intensity-weighted hydrodynamic radius (R_H) and scattering intensity and ξ of the silica particles in the water solution on a Zetasizer NanoZS instrument, model ZEN3600 (Malvern Instruments, Malvern, UK) at the temperature of 25 °C [27]. R_H was measured at a scattering angle of $\theta = 173°$, and the data were processed with the REPES algorithm [28]. The zeta potential data were evaluated using the Smoluchowski model [29].

2.6. Scanning electron microscope

SEM micrographs were taken with an electron microscope Vega TS 5135 at 30 kV acceleration voltage, magnification 5000 times. Pure silicon oxide (SiO_2) and core-shell nanoparticles were measured after placing them on carbon tape without the necessity of any metal sputtering.

2.7. Transmission electron microscope

TEM observations were performed through a Tecnai G2 Spirit Twin 12 (FEI, Czech Republic), using a bright field imaging mode at an accelerating voltage of 120 kV.

3. Results and discussion

3.1. Size analysis

We have covered relatively large SiO_2 NPs of diameter 0.961 ± 0.046 μm (minimum size 0.804 μm, median 0.962 μm, maximum size 1.077 μm, 696 counts, Fig. 1a) with polydopamine forming core-shell NPs of 1.019 ± 0.058 μm diameter (minimum size 0.835 μm, median 1.021 μm, maximum size 1.198 μm, 495 counts, Fig. 1b). The difference in the average size of coated and uncoated particle diameter is 58 nm. The thickness of the PDA layer is half of this value which is ca. 29 nm. For all other presented parameters differences are following minimum size of 31 nm, median of 59 nm, and maximum size of 121 nm. The analysis of variance (ANOVAOneWay, Origin 2019) on raw data, has shown that the difference of means is significant at the level $p = 0.001$ in seven statistical tests performed (details see SI).

The dynamic light scattering data presented in Fig. 2 shows differences in size distributions although it measures hydrodynamic radius which is slightly larger than obtained from SEM measurements. The original silica particles dispersed in the solution show particles with the size $R_H = 470$ nm. The silica covered by PDA demonstrates more scattering particles with the size $R_H = 550$ nm. The scattering intensity increased from 4000 kHz to 12,000 kHz, so three times. Data are well reproducible and presented in Fig. 2. Fig. 1c and d show TEM images of PDA@SiO_2 particles with a special focus on the PDA layer. The thickness of PDA taken from 193 random measurements all over the surface is 27.9 ± 25.8 nm (minimum thickness is 2.5 nm, maximum thickness is 182.9 nm, statistics Fig. S7).

The growth of the particles after covering is in perfect agreement with SEM measurements. As we consider the hydrodynamic radius, the structured solvent layer we have to take into attention. The zeta potential measurements performed on the same sample during the same experimental sequence are represented in Fig. 2 inset. Original silica particles were charged ($\xi = -65$ mV). After covering by PDA, the surface charge of silica particles is compensated, and covered particles are electrically neutral. The thickness of the PDA layer is around 50–80 nm.

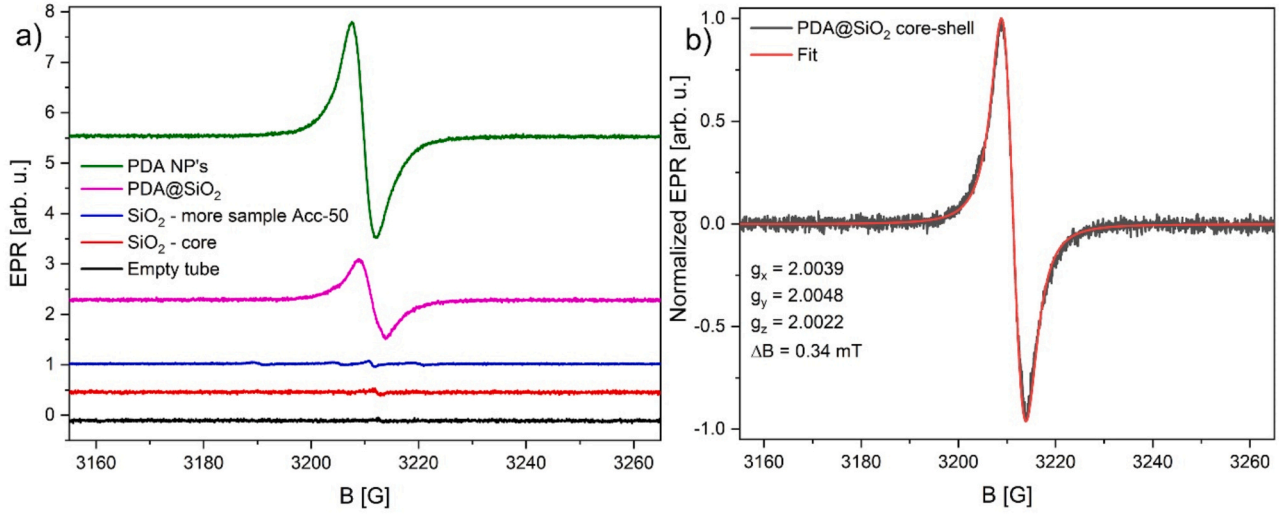

Fig. 3. a) EPR signal of from bottom empty tube; SiO_2 nanoparticles - the core of core-shell structure; the same nanoparticles but 5 times more accumulation 100 times more sample; core-shell structure PDA@SiO_2 NP's, pure PDA nanoparticles; b) Normalized EPR signal of PDA@SiO_2 core-shell nanoparticles.

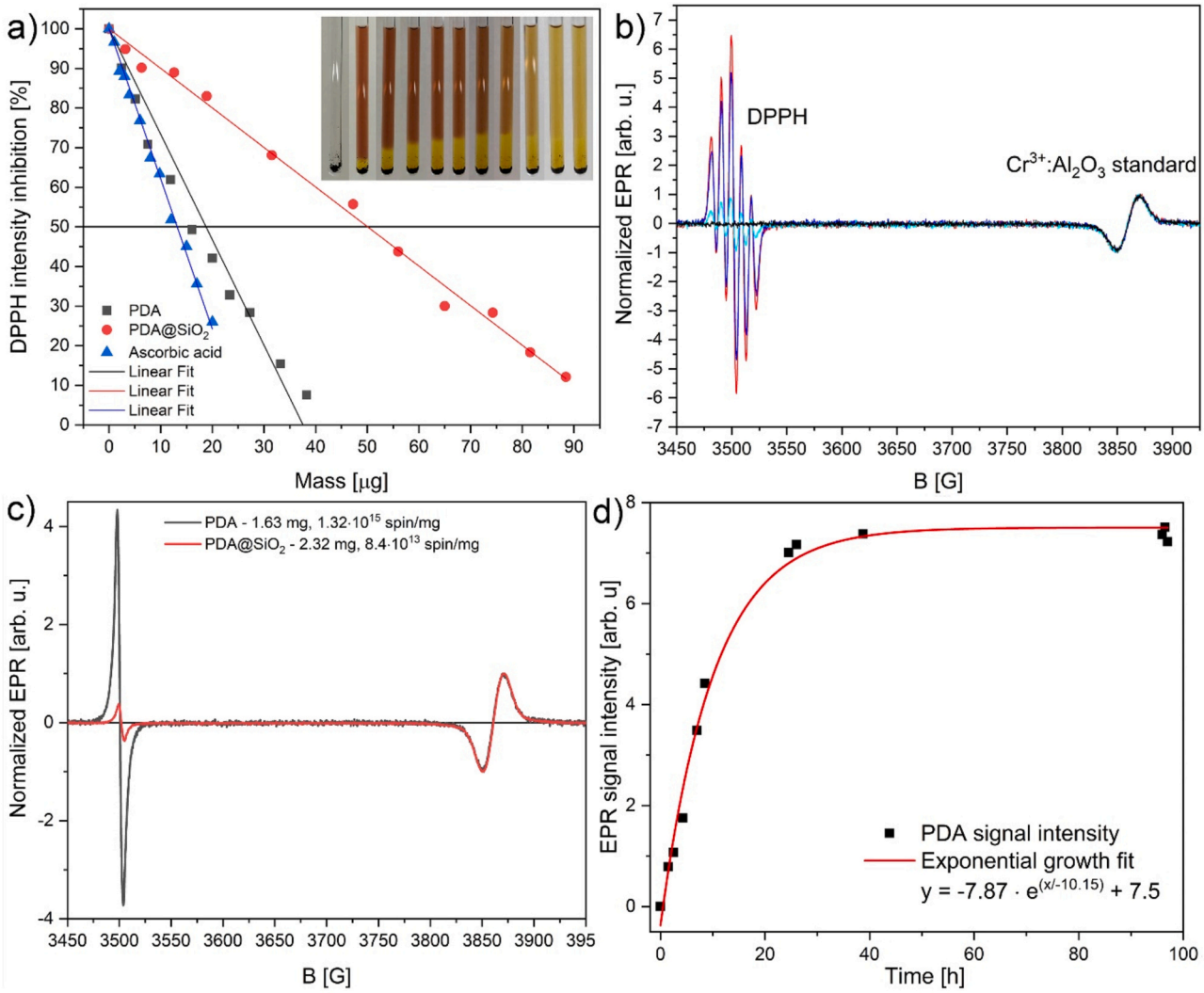

Fig. 4. a) EPR radical scavenging experiment - DPPH signal inhibition for rising masses of: PDA (black), PDA@SiO_2 (red), ascorbic acid standard (blue); Inset shows PDA powder in EPR tube that scavenges DPPH ethanol/water solution during 8 h; b) Decrease of DPPH signal in time after the addition of PDA; Cr^{3+}:Al_2O_3 is a spin concentration standard mounted on the resonators wall (previously calibrated with alanine standard and normalized to ± 1 amplitude, constant during the entire experiment); c) Exemplary EPR spectra of PDA showing stationary state DPPH signals for various PDA masses; d) Increase of PDA signal intensity measured by EPR spectroscopy during the entire process of dopamine polymerization.

3.2. Electron paramagnetic resonance

Electron paramagnetic resonance spectroscopy provides a vast amount of information about the paramagnetic centers in materials among them are a concentration of radicals, number of different radicals, g-factors and hyperfine constants related to radical's local side symmetry, line widths related to relaxation rates, or finally stability of them in various conditions. EPR is sensitive enough to use its signal as a marker of local dynamics e.g. Jahn–Teller effect [30], and structural changes e.g. phase transitions [31,32]. Polydopamine shows at least two persistent, overlapping EPR signals coming from two radicals which can be distinguished in low temperatures in pulsed EPR measurements [19] or continuous wave saturation experiments [33,34].

Core-shell structure poses a similar EPR signal to the pristine PDA NPs. The pristine PDA nanoparticles were obtained in the same conditions as PDA@SiO_2 core-shell nanoparticles but without the introduction of SiO_2 nanoparticles during polymerization.

A comparison of them can be found in SI. Fig. 3a shows the EPR signals of all components. The core SiO_2 particle exhibits a very weak radical signal which is only visible after measuring ten times larger amount of the sample in the tube together with 50 accumulations (instead of 5 as before). If measuring a similar quantity of powder as for PDA@SiO_2 sample the EPR core signal is simply lacking. The EPR signal could be fitted with a single Lorentz function ($\Delta B = 0.34$ mT) with g-tensor anisotropy [2.0039, 2.0048, 2.0022], and small g-strain resulting from the inhomogeneity of the material (EasySpin, pepper subroutine) showing very good fidelity (Fig. 3b). Very similar fitting parameters show PDA NPs, which fit can be found in SI.

Fig. 4a depicts how a specific mass of PDA and PDA@SiO_2 is able to scavenge DPPH molecules. With increase of the NPs mass this effect becomes stronger. In this reaction, DPPH gains additional hydrogen and forms DPPH-H. With this process, radical (unpaired electron) located at the DPPH molecule vanishes. The same process can be observed using absorbance spectroscopy in the UV-Vis range where the decolorization of the solution is observed from initial deep purple to yellow color (517 nm). The results show that for converting 1 mmol of DPPH molecules into DPPH-H moieties it is necessary to use 107.15 μg of PDA NPs, 310.59 μg PDA@SiO_2 core-shell NPs, and used as control in this experiment 72.55 μg of ascorbic acid. The ED_{50} doses are half of the measured values for PDA - 53.5 μg/mmol of DPPH molecules, for PDA@SiO_2 - 155.3 μg/mmol, and for ascorbic acid 36.2 μg/mmol of DPPH. These values are slightly higher than those presented in the introduction, but

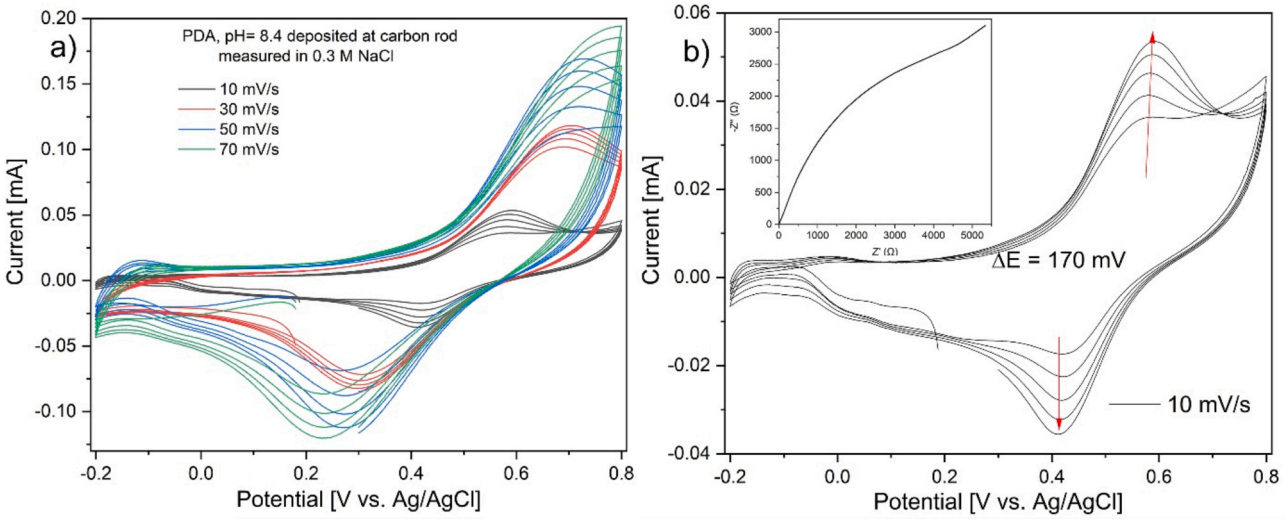

Fig. 5. a) Cyclic voltamperometry of PDA@SiO_2 for various cycling speeds 10, 30, 50, 70 mV/s; b) Cyclic voltammetry of 10 mV/s scan rate (the red arrows show an increase of cathodic and anodic currents under multiple cycles, inset shows the plot of imaginary vs. real part of impedance.

different values can be solvent dependent. The Scavenging capacity of PDA is comparable with the activity of ascorbic acid and is at the level of 67.7 % of it. This makes PDA a very potent radical scavenger. The inset shown in Fig. 4a depicts one-dimensional diffusion driven reaction of PDA with DPPH forming DPPH-H which was registered 8 h long. The reaction rate in this case is equal to the transport rate of the DPPH molecules moving down to the bottom of the tube where PDA powder remains. These molecules move much faster than NPs through the solution. For scavenging experiments, vials were vigorously stirred (1 h) to reach faster the steady state conditions. Fig. 4b depicts the decrease of DPPHs EPR signal after admixing the increasing mass of PDA NPs. The spin concentration measured in Fig. 4c was measured by a simultaneous experimental method by comparison with chromium-doped standard. The PDA sample showed $1.32 \times 10^{15} spin/mg$ while for sample PDA@-SiO_2 it is $8.4 \times 10^{13} spin/mg$ (Fig. 4c). Fig. 4d shows the growth in time of PDA signal during polymerization reaction while constantly stirring and up taking 20 µl for EPR measurement. The stabilization of the signal intensity (steady-state conditions) informs of the end of the polymerization, after around 48 h.

3.3. Electrochemistry

To study the electrochemical performance of PDA@SiO_2 NPs the thin film was deposited on carbon rods and two main methods were applied: cyclic voltammetry in potential window range from − 0.2 V to 0.8 V vs Ag/AgCl (3 M KCl) reference electrode with different scan rates (see Figs. 5a and 5b) and electrochemical impedance spectroscopy recorded at open circuit potential (see inset Fig. 5b).

According to the CV measurements, only one oxidation and one reduction peak is recorded (Fig. 5a). The peak-to-peak potential separation ΔE is 170 mV for 10 mV/s scan rate (Fig. 5b) and increases with the increasing scan rate, which means that oxidation and reduction processes are quasi-reversible in our systems. The higher separation of ~ 400 mV at a 5 mV/s scan rate was recorded by M.T. Cortes and *co-authors* for PDA prepared in TRIS buffer [35]. Based on the literature data and comparing it with the CV measured for PDA@SiO_2 films we conclude that PDA@SiO_2 films have a quasi-reversible electrochemical response, which is stable and not electrochemically degradable. Such a system could be applied in sensor applications. Also, the oxidation current is higher compared to the reduction current even for the lowest scan rate. The scan rate of 70 mV/s has the same current values as 50 mV/s. This could be explained by the diffusion processes at such surfaces. Another interesting observation was recorded: for each scan rate it is observed that with the increasing number of the same scan rate the current gradually increases (anodic and cathodic), for more details see Fig. 5b. This fact could be explained by the percolation of ions (in our case the measurements were done in 0.3 M NaCl) and involving more electroactive material in oxidation/reduction processes. The opposite effect was recorded and published by R.A. Zangmeister and co-authors – with an increasing number of CV measurements the oxidation/reduction currents decreased [36]. The electrochemical impedance spectroscopy confirms that PDA@SiO_2 film has charge transfer resistance ~ 1 kΩ, which is connected with the way PDA is attached to SiO_2 spheres, and how these nanoparticles interact with each other (Fig. 5b inset).

4. Conclusions

We have successfully covered large silica nanoparticles (ca. 960 nm) with a thin ca. 29 nm layer of polydopamine. The spin concentration of PDA NPs was estimated for $1.32 \times 10^{15} spin/mg$ (synthesis without SiO_2 NPs), and for the core-shell system - PDA@SiO_2 it was $8.4 \times 10^{13} spin/mg$. Both systems pure PDA NPs and core-shell showed radical scavenging properties. To eliminate 1 mmol of DPPH radicals it was necessary to use 107.15 µg of PDA, and 310.59 µg PDA@SiO_2. Electrochemical properties are similar to pristine PDA nanoparticles. It was shown that the dopamine polymerization reaction ends after ca. 48 h held in an open, vigorously stirred, beaker. PDA@SiO_2 films have a quasi-reversible electrochemical response, which is stable and not electrochemically degradable. The peak-to-peak potential separation ΔE is 170 mV for a 10 mV/s scan rate which is less than reported elsewhere. Anodic and cathodic currents are gradually increasing with the increase of the scan rate. Both conclusions imply a stabilizing effect on the PDA layer coming from the SiO_2 core. The reported system is suitable for sensor applications.

CRediT authorship contribution statement

Krzysztof Tadyszak: Conceptualization, measurements: EPR, SEM, text corrections. **Elena Tomšík:** measurements: electrochemistry, text corrections, Formal analysis. **Zulfiya Černochová:** measurements: DLS, text corrections, Formal analysis.

Declaration of Competing Interest

The authors declare the following financial interests/personal relationships which may be considered as potential competing interests:

Krzysztof Tadyszak reports financial support was provided by Ministry of Education, Youth and Sports of the Czech Republic and Czech Science Foundation.

Data availability

Data will be made available on request.

Acknowledgement

We acknowledge the financial support from the Ministry of Education, Youth and Sports of the Czech Republic (grant no. LM2023053), and the Czech Science Foundation (grant no. 21-01090S). We are grateful to Mgr. Jiřina Hromádková for performing the TEM measurements.

Appendix A. Supporting information

Supplementary data associated with this article can be found in the online version at doi:10.1016/j.synthmet.2023.117492.

References

[1] W.-B. Tsai, W.-T. Chen, H.-W. Chien, W.-H. Kuo, M.-J. Wang, Poly(dopamine) coating of scaffolds for articular cartilage tissue engineering, Acta Biomater. 7 (2011) 4187–4194.
[2] Y. Kim, et al., Efficient photocatalytic production of hydrogen by exploiting the polydopamine-semiconductor interface, Appl. Catal. B Environ. 280 (2021), 119423.
[3] M.E. Lynge, R. van der Westen, A. Postma, B. Städler, Polydopamine—a nature-inspired polymer coating for biomedical science, Nanoscale 3 (2011) 4916–4928.
[4] R. Luo, et al., Improved immobilization of biomolecules to quinone-rich polydopamine for efficient surface functionalization, Colloids Surf. B Biointerfaces 106 (2013) 66–73.
[5] J. Cui, et al., Immobilization and intracellular delivery of an anticancer drug using mussel-inspired polydopamine capsules, Biomacromolecules 13 (2012) 2225–2228.
[6] P. He, et al., Functionalized nano-SiO2 for improving the cycling stability of 4.6V high voltage LiCoO2 cathodes, Electrochim. Acta 427 (2022).
[7] K. Tadyszak, et al., Spectroscopic and magnetic studies of highly dispersible superparamagnetic silica coated magnetite nanoparticles, J. Magn. Magn. Mater. 433 (2017).
[8] A. Jędrzak, et al., Dendrimer based theranostic nanostructures for combined chemo- and photothermal therapy of liver cancer cells in vitro, Colloids Surf. B Biointerfaces 173 (2019) 698–708.
[9] P. Meredith, T. Sarna, The physical and chemical properties of eumelanin, Pigment Cell Res. 19 (2006) 572–594.
[10] H. Liu, et al., Role of polydopamine's redox-activity on its pro-oxidant, radical-scavenging, and antimicrobial activities, Acta Biomater. 88 (2019) 181–196.
[11] R. Mrówczyński, et al., Electron paramagnetic resonance imaging and spectroscopy of polydopamine radicals, J. Phys. Chem. B 119 (2015).
[12] K.-Y. Ju, Y. Lee, S. Lee, S.B. Park, J.-K. Lee, Bioinspired polymerization of dopamine to generate melanin-like nanoparticles having an excellent free-radical-scavenging property, Biomacromolecules 12 (2011) 625–632.
[13] J. Hu, et al., Polydopamine free radical scavengers, Biomater. Sci. 8 (2020) 4940–4950.
[14] H. Lee, B.P. Lee, P.B. Messersmith, A reversible wet/dry adhesive inspired by mussels and geckos, Nature 448 (2007) 338–341.
[15] R. Mrówczyński, R. Turcu, C. Leostean, H.A. Scheidt, J. Liebscher, New versatile polydopamine coated functionalized magnetic nanoparticles, Mater. Chem. Phys. 138 (2013) 295–302.
[16] S. Palanisamy, Polydopamine supported gold nanoclusters for sensitive and simultaneous detection of dopamine in the presence of excess ascorbic acid and uric acid, Electrochim. Acta 138 (2014) 302–310.
[17] M. Zhu, et al., A cytocompatible conductive polydopamine towards electrochromic energy storage device, Electrochim. Acta 374 (2021), 137961.
[18] B.-L.L. Seagle, et al., Time-resolved detection of melanin free radicals quenching reactive oxygen species, J. Am. Chem. Soc. 127 (2005) 11220–11221.
[19] K. Tadyszak, R. Mrówczyński, R. Carmieli, Electron spin relaxation studies of polydopamine radicals, J. Phys. Chem. B (2021), https://doi.org/10.1021/acs.jpcb.0c10485.
[20] M. Pasenkiewicz-Gierula, R.C. Sealy, Analysis of the ESR spectrum of synthetic dopa melanin, Biochim. Biophys. Acta Gen. Subj. 884 (1986) 510–516.
[21] B.L. Seagle, K.A. Rezai, Y. Kobori, E.M. Gasyna, K.A. Rezaei, J.J. N, Melanin photoprotection in the human retinal pigment epithelium and its correlation with light-induced cell apoptosis, Proc. Natl. Acad. Sci. USA 102 (2005) 8978–8983.
[22] M.S. Blois, A.B. Zahlan, J.E. Maling, Electron spin resonance studies on melanin, Biophys. J. 4 (1964) 471–490.
[23] H.S. Mason, D.J.E. Ingram, B. Allen, The free radical property of melanins, Arch. Biochem. Biophys. 86 (1960) 225–230.
[24] M. d'Ischia, A. Napolitano, A. Pezzella, P. Meredith, T. Sarna, Chemical and structural diversity in eumelanins: unexplored bio-optoelectronic materials, Angew. Chem. Int. Ed. 48 (2009) 3914–3921.
[25] Y. Jing, et al., Ultrathin two-dimensional polydopamine nanosheets for multiple free radical scavenging and wound healing, Chem. Commun. 56 (2020) 10875–10878.
[26] R. Micillo, et al., Unexpected impact of esterification on the antioxidant activity and (photo)stability of a eumelanin from 5,6-dihydroxyindole-2-carboxylic acid, Pigment Cell Melanoma Res. 31 (2018) 475–483.
[27] I. Brezaniova, et al., Self-assembled chitosan-alginate polyplex nanoparticles containing temoporfin, Colloid Polym. Sci. 295 (2017) 1259–1270.
[28] J. Jakeš, Regularized positive exponential sum (REPES) program - a way of inverting laplace transform data obtained by dynamic light scattering, Collect. Czech. Chem. Commun. 60 (1995) 1781–1797.
[29] F. Jüttner, Jena Bearbeitet von F. Auerbach, K. Baedecker Jena, A. Becker Heidelberg, E. Bräuer Voigtsdorf, P Cermak Gießen, H. Diesselhorst Braunschweig, A. Eichenwald Moskau, G. Gehlhoff Berlin, E. Gehrke Ch., Handbuch der Elektrizität und des Magnetismus, Z. Elektrochem. Angew. Phys. Chem. 30 (1924) 296A–297A.
[30] S.K. Hoffmann, J. Goslar, K. Tadyszak, Electronic structure and dynamics of low symmetry Cu2+ complexes in kainite-type crystal KZnClSO4·3H2O: EPR and ESE studies, J. Magn. Reson. 205 (2010) 293–303.
[31] N.A. Wojcik, et al., Tunable dielectric switching of (quinuclidinium)[MnCl4] hybrid compounds, J. Phys. Chem. C 125 (2021) 16810–16818.
[32] A. Ostrowski, W. Bednarski, High temperature phase transition and multiphase state formation in K3H(SO4)2 superprotonic conductor, Solid State Ion. 301 (2017) 152–155.
[33] A.B. Mostert, S.B. Rienecker, C. Noble, G.R. Hanson, P. Meredith, The photoreactive free radical in eumelanin, Sci. Adv. 4 (eaaq1293) (2023).
[34] A.B. Mostert, et al., Hydration-controlled X-band EPR spectroscopy: a tool for unravelling the complexities of the solid-state free radical in eumelanin, J. Phys. Chem. B 117 (2013) 4965–4972.
[35] M.T. Cortés, et al., Bioinspired polydopamine synthesis and its electrochemical characterization, J. Chem. Educ. 96 (2019) 1250–1255.
[36] R.A. Zangmeister, T.A. Morris, M.J. Tarlov, Characterization of polydopamine thin films deposited at short times by autoxidation of dopamine, Langmuir 29 (2013) 8619–8628.